

## Supplementary Information

### Site Descriptions

The coordinates of the three L.A. Megacity Carbon Project sites and MWO are provided in Table 1 of Verhulst et al. (1). The air intake at GRA is located 51 m above ground level (agl) on a cell phone tower in the San Fernando Valley; at USC air is drawn in from a mast on the corner of a tall building on the campus of the University of Southern California, leading to a total inlet height of 50 m agl; the same is the case for FUL at California State University, Fullerton. For the latter two cases, the buildings are among, if not, the tallest buildings on the campus, standing out substantially from the other buildings and were chosen because of these characteristics. MWO has a relatively short inlet (3 m agl) but lies atop a tall ridge (1670 m above sea level) above the L.A. Basin. In order to avoid polluted Basin air brought to the site by upslope winds during day time, air samples for CO<sub>2</sub> and Δ<sup>14</sup>C analysis were collected exclusively at night when the site is exposed to air from the overlying free troposphere.

### Uncertainty in C<sub>ff</sub> and C<sub>bio</sub>

Random error in C<sub>ff</sub> and C<sub>bio</sub> is calculated by propagating the following uncertainties through eq. 3 (C<sub>ff</sub>) and eq. 1 (C<sub>bio</sub>) in the main text. We assume the following random errors for individual terms: C<sub>obs\_err</sub> = 0.1 ppm (CO<sub>2</sub> measurement precision); C<sub>bg\_err</sub> =  $\sqrt{(C_{bg\_fit\_err}^2 + C_{obs\_err}^2)}$  = 0.9 ppm (where C<sub>bg\_fit\_err</sub> = 0.9 ppm and is the standard deviation of differences between selected (“clean”) MWO observations and their smooth curve fit); Δ<sub>obs\_err</sub> = 1.8 ‰ (Δ<sup>14</sup>C measurement precision); Δ<sub>bg\_err</sub> =  $\sqrt{(\Delta_{bg\_fit\_err}^2 + \Delta_{obs\_err}^2)}$  = 2.2 ‰ (where Δ<sub>bg\_fit\_err</sub> = 1.3 ‰ and is the standard deviation of differences between selected MWO observations and their smooth curve fit). The second term in eq. 3 in the main text, representing biospheric “disequilibrium flux” is given an uncertainty of 100%, which is 0.25 ppm. Using a Monte Carlo approach with 10,000 trials, we calculate the 1 σ standard deviation of C<sub>ff</sub> and obtain C<sub>ff\_err</sub> = 1.2 ppm. Then, we calculate the 1 σ standard deviation of C<sub>bio</sub> and obtain C<sub>bio\_err</sub> = 1.5 ppm. Error bars of this size appear in the top panel of Fig. 4 when displaying C<sub>bio</sub>. To calculate monthly medians and associated 95% confidence intervals for C<sub>bio</sub>, we perform a bootstrap uncertainty calculation. We randomly select from all the C<sub>bio</sub> values for a given month a number of samples equal to the original number, allowing for a given C<sub>bio</sub> value to be selected multiple times (i.e. “bootstrap, with replacement”). During each random selection we also add a random number to C<sub>bio</sub> consistent with the 1.5 ppm random uncertainty obtained above. Then, the mean C<sub>bio</sub> value is calculated for the month under consideration. This process is repeated 1000 times and the median, 2.5th and 97.5th percentiles of the 1000 member distribution are reported in the top panel of Figure 4 (red symbols and error bars). The same bootstrapping approach is used to calculate medians and 95% confidence intervals for the values in Figure 5, where the uncertainty on individual values is 28%, based on propagation of random error in C<sub>xs</sub> and C<sub>ff</sub>.

### Windspeed and direction filtering

After applying wind direction filtering and our preferred wind speed criteria, 83%, 86% and 54% of data were retained at GRA, USC, and FUL, respectively. Use of a higher windspeed filter

threshold of  $2.0 \text{ ms}^{-1}$  had little impact on the results (Table S1), although the percentage of data retained for analysis changed to 73%, 83%, and 22%.

## Mixing Line Analysis

To determine the time-independent, aggregate, fractional fossil and biogenic contributions to  $C_{xs}$   $f_{ff}$  and  $f_{bio}$  (where  $f_{ff} + f_{bio} = 1$ ), we conduct a two end-member mixing analysis based on the following equation:  $\Delta_{source} = f_{ff} \times \Delta_{ff} + f_{bio} \times \Delta_{bio} = f_{ff} \times \Delta_{ff} + (1 - f_{ff}) \times \Delta_{bio}$ .  $\Delta_{source}$  is the slope of the mixing line (-783 ‰) as determined via the methods described below and in the main text,  $\Delta_{ff} = -1000$  ‰ and  $\Delta_{bio} = -16.5$  ‰. As stated in the main text,  $\Delta_{bio}$  is assumed equal to  $\Delta_{obs}$ , the mean atmospheric non-background  $\Delta^{14}C$ .  $\Delta_{bio}$  is the isotopic signature of  $C_{bio}$ , which is  $C_r + C_p$ . The assumption that  $\Delta_{bio} = \Delta_{obs}$  is not completely accurate. In fact we can only say that  $\Delta_{bio} = \Delta_p$ , because there is an isotopic disequilibrium associated with respiration,  $r$ . However, the impact of this approximation is small. Using our rather large estimate of isotopic disequilibrium of +50 ‰, this would make  $\Delta_r = +33.5$  ‰, yielding an (unweighted)  $\Delta_{bio} \sim +8.5$  ‰. Using the simple (-16.5 ‰) or disequilibrium corrected value (+8.5 ‰) of  $\Delta_{bio}$  yields values for  $f_{ff}$  and  $f_{bio}$  of either 77.9 % and 22.1 % (simple) or 78.5 % and 21.5 % (disequilibrium corrected).

## Calculation of biogenic:fossil emission ratios.

### A. Economic activity sectors

We use the breakdown of sectoral emissions into biogenic and fossil components that exists at the state level to compute an overall Southern California biogenic:fossil emission ratio for “economic” emission sectors (i.e. excluding human respiration and excretion). As can be seen in Table S2, statewide biogenic:fossil ratios are multiplied by Southern California fossil emissions (available from the Vulcan Project), to obtain Southern California biogenic fluxes. Southern California fossil and biogenic emissions are then totaled and ratioed to obtain the Southern California biogenic:fossil emission ratio. As a sensitivity test (see below), we also use the biogenic:fossil ratios for different activity sectors for Southern California counties from the newly available ACES inventory (updated from ref. 2).

### B. Human metabolism

Human respiration and excretion represent a major category of  $CO_2$  emissions in urban areas. At national and international scales, these positive fluxes to the atmosphere are balanced by photosynthetic uptake by crops that act as a direct (or indirect via meat consumption) source of calories. However, in urban regions such as the Los Angeles area, the great majority of carbon efflux from human beings was originally taken up as  $CO_2$  in outlying rural areas. We calculate the ratio of human metabolic (respiratory plus excretory):fossil emissions using fossil emissions for Southern California from Vulcan 3.0 (after correcting for biogenic on-road emissions) and derive human emissions from the work of Prairie and Duarte (3). Using a global population of  $6.1 \times 10^9$  and average human mass of 70 kg, they derive respiratory and excretory emissions of 257 and 128 gC/person/day, respectively, for a total of 385 g C/person/day. In Table S3, we use this emission rate and the populations of the five Southern California counties to calculate human  $CO_2$  emissions per county. The total five-county human and fossil emissions are then ratioed to give a ratio 0.057.

## Sensitivity of $C_{\text{bio}}$ to bio:fossil emission ratios

We also performed a sensitivity test in the calculation of  $C_{\text{bio}}$  in which we use biogenic:fossil emission ratio of 0.107 (0.050 + 0.057) instead of the value 0.160 used in the main text. Here, the value of 0.050 for biogenic:fossil emissions from fuel sectors (instead of 0.103; see Table S1) comes from the biogenic:fossil emissions ratio from the newly available ACES inventory (2). Figure S2 shows a comparison of  $C_{\text{bio}}$  with the original biogenic:fossil emission ratios and the modified one. The modified version shows monthly mean values of  $C_{\text{bio}}$  that are more positive by  $0.67 \pm 0.13$  ppm, but the amplitude of the seasonal cycle is largely unchanged, but with both “zero-crossing” dates closer to the date of the minimum.

## Sensitivity to Background

If we were to use the high-altitude continental site NWR instead of MWO as a background site, annual average  $C_{\text{xs}}$  increases from 14.8 to 16.1 ppm with the increase of 1.3 ppm split evenly between  $C_{\text{ff}}$  and  $C_{\text{bio}}$ . Annual  $C_{\text{ff}}$  changes from  $13.0 \pm 2.8$  ppm to  $13.7 \pm 2.7$  ppm (annual mean and standard deviation of monthly mean  $C_{\text{ff}}$ ) and annual  $C_{\text{bio}}$  changes from  $1.5 \pm 1.9$  to  $2.3 \pm 1.4$  ppm.  $\Delta_{\text{source}}$  (when all sites are binned) changes from  $-783 \pm 11$  ‰ to  $-787 \pm 10$  ‰ when using NWR instead of MWO. There are also monthly effects in our choice of background as can be seen in the differing values of  $C_{\text{bio}}$  in June and November (Figure S2). The seasonal amplitude of the  $C_{\text{bio}}$  seasonal cycle (calculated as the mean of the three highest consecutive months, November through January, minus the mean of the three lowest consecutive months, June through August) is reduced from 4.3 ppm to 2.6 ppm when using NWR as background. This effect results from differences in the seasonal cycles of both  $\text{CO}_2$  and  $\Delta^{14}\text{C}$  at the two sites (Figure S3). Nonetheless, as stated in the main text, MWO is the clear preference as a background site for this study because of its far greater proximity to FUL, USC and GRA in the L.A. megacity.

Despite  $\Delta^{14}\text{C}$  data from Utqiagvik, AK (BRW) having been previously used to represent background for L.A. Basin measurements (4), we chose not to test the sensitivity of our calculations to BRW  $\Delta^{14}\text{C}$ . BRW is too remote of a site from Los Angeles to test as background, given that we have available data from MWO (and NWR). Note that in the case of the Newman et al. study (4), BRW represented the only available background time series.

## Eddy covariance data from Southern California

Monthly mean net ecosystem exchange (NEE) calculated by eddy covariance in surrounding unmanaged Southern California ecosystems including those classified as “Sage”, “Grassland”, “Pinyon/Juniper”, “Desert” and “Oak/Pine” from the Southern California Climate Gradient study are shown in Figure S4. Monthly means are calculated using 30-minute gap-filled data obtained from the Ameriflux website (<https://ameriflux.lbl.gov/>). The time spans for the different sites are Sage: March 27, 2006 – Oct. 4, 2016; Grassland: March 17, 2016 – Oct. 4, 2016; Pinyon/Juniper: May 17, 2016 – Oct. 4, 2016; Desert: April 21, 2006 – March 16, 2014; Oak/Pine: Sept. 12, 2006 – Jan. 11, 2015. Sage, Grassland and Pinyon/Juniper sites show climatological minima (maximum C uptake) in March/April, following the climatological winter rainy season (Figure 4 and Figure S4). Only the climatological NEE signal from Oak/Pine shows a phasing similar to

the  $C_{bio}$ ' signal we observe in the L.A. Basin, with maximum uptake in June. The Oak/Pine eddy flux site sits at the highest elevation (1770 m a.s.l.) of all the Southern California Climate Gradient study sites and is a deeply rooted evergreen forest and is thus less sensitive to winter/spring rain than the deciduous vegetation at lower elevations. Also note that absolute values of NEE at the Oak/Pine site showing sink behavior in all months of the year are unrealistic and likely have to do with nighttime drainage of air down slopes.

### Tree and Turf Cover

Figure S6 shows a composite image of Southern California tree and turf cover aggregated to a resolution of 0.03 degrees, the resolution of our WRF-STILT footprints. The map in Figure S6 is composed of a high-resolution ( $\sim 0.00038$  degrees for latitude and longitude) map of landcover classification obtained using the AVIRIS airborne spectrometer (5) for the urban regions of the L.A. Basin. Landcover is classified into tree, turf, soil, non-photosynthetic vegetation, paved and roof fractions. Here we combine the tree and turf classes into a live vegetation fraction. For the parts of our domain (defined by the footprint extent) where these data did not exist, we used the tree and grass fraction the MODIS Vegetation Continuous Fields (VCF, product MOD44bv6 (6)) which has a native resolution of 250 m. In order to calculate the mean vegetation fraction in the footprint of our measurements, we convolved WRF-STILT footprints with the combined vegetation fraction map (both at 0.03 degrees latitude x longitude) for each air sample as

$$Vfrac = \frac{\sum Veg\_fraction\_map \times Footprint}{\sum Footprint}$$

The means and standard deviations (over time) of this footprint-weighted vegetation fraction for USC, GRA, and FUL are, respectively,  $13.6 \pm 2.1\%$ ,  $14.6 \pm 4.4\%$ , and  $14.6 \pm 2.3\%$ .

### Contribution of high-altitude tree ecosystems to observed $C_{bio}$ '

Figure S7 shows a comparison of  $C_{bio}$ ' as inferred from Los Angeles  $\Delta^{14}C$  and  $CO_2$  measurements (blue line; identical to that in Figure 4) with locally added biospheric  $CO_2$  from high altitude forest ecosystems within the footprint of GRA, USC and FUL (red and black lines). These estimates of forest  $C_{bio}$ ' were calculated by first assuming that all pixels (0.03 x 0.03 degree) in our domain with elevations greater than 1500 m asl had the NEE seasonality of the Oak/Pine eddy flux site (Figure S4). Then, this flux field was convolved with either a) individual footprints from all the sites (black line) and then averaged or b) the sum of the annual average footprints for each site (Figure 1) (red line). The tree fraction in each pixel, as determined from MODIS VCF (see SI text and Figure S6), was used to scale the NEE. To remove the artifacts in the eddy flux NEE data likely associated with nighttime drainage that produce an unrealistic sink in every month, the annual mean NEE was subtracted from the NEE shown in Fig. 2 before convolution, but this did not affect the amplitude of simulated  $C_{bio}$ '. The amplitude of both the black and red lines is far smaller than that of observed  $C_{bio}$ '.

## Curve fitting

### *Background*

A second order polynomial plus four harmonics are fit to the selected MWO data. Following the method of Thoning et al. (7), data residuals from the curve fit are filtered with a “cutoff 1” low pass filter of 80 days, and the smoothed residuals are added back to the original curve fit. The 80-day low-pass filter has a full-width half-maximum of 47 days in the time domain.

### *Isotopic Mixing plot*

Following the method of York et al. (8, see also 9), we regress  $C_{xs}$  vs.  $(\Delta \times C)_{xs}$  accounting for measurement errors for both  $\text{CO}_2$  and  $\Delta^{14}\text{C}$  and correlation between x and y errors, because  $\text{CO}_2$  appears in both the ordinate and abscissa. Measurement errors are scaled so that reduced chi-squared is one, and then the final value of the slope and intercept errors are calculated. This chi-squared scaling does not affect the slope, however, because the ratio of the x and y errors is kept constant.

**Table S1. Impact of Windspeed Threshold**

<b>Quantity</b>	<b>1.5 ms<sup>-1</sup></b>	<b>2.0 ms<sup>-1</sup></b>	<b>Unit</b>
Average CO <sub>2xs</sub>	14.6 ± 11.8	14.8 ± 12.2	ppm
Average Δ <sup>14</sup> C <sub>xs</sub>	-30.9 ± 21.4	-31.1 ± 22.2	‰
C <sub>xs</sub> vs. (Δ × C) <sub>xs</sub> R <sup>2</sup>	0.94	0.95	none
C <sub>xs</sub> vs. (Δ × C) <sub>xs</sub> slope all sites	-783 ± 11	-795 ± 12	‰
C <sub>xs</sub> vs. (Δ × C) <sub>xs</sub> slope GRA	-786 ± 18	-798 ± 20	‰
C <sub>xs</sub> vs. (Δ × C) <sub>xs</sub> slope USC	-758 ± 19	-761 ± 19	‰
C <sub>xs</sub> vs. (Δ × C) <sub>xs</sub> slope FUL	-787 ± 30	-814 ± 50	‰
C <sub>ff</sub>	13.2 ± 9.4	13.3 ± 9.8	ppm
C <sub>ff</sub> summer	14.0 ± 12.7	13.6 ± 13.6	ppm
C <sub>ff</sub> winter	13.2 ± 6.9	13.4 ± 6.5	ppm
C <sub>bio</sub>	1.5 ± 1.9	1.5 ± 1.9	ppm
C <sub>bio</sub> summer	-0.2 ± 1.2	-0.3 ± 1.0	ppm
C <sub>bio</sub> winter	3.6 ± 0.9	3.5 ± 0.9	ppm

**Table S2. Biogenic:Fossil emissions and ratios for economic sectors**

<b>Sector</b>	<b>State Bio:Fossil<sup>1</sup></b>	<b>So. Cal. Fossil<sup>2,3</sup></b>	<b>So. Cal. Bio<sup>2,3</sup></b>
Residential	0.132	2.85	0.375
Commercial	0.046	2.46	0.113
Industrial	0.166	11.48	1.912
Electricity Production <sup>4</sup>	0.148	5.47	0.809
On-road	0.072 <sup>5</sup>	19.47	1.501
Non-road	0.000	1.64	0.000
Airport <sup>6</sup>	0.003	0.89	0.003
Rail	0.000	0.47	0.000
CMV <sup>7</sup>	0.010	0.48	0.005
Cement <sup>8</sup>	0.000	0.51	0.000
<b>Total</b>	<b>0.103</b>	45.72	4.718

1. State bio/fossil emission ratios are from California Air Resources Board (CARB) statewide data for 2015. Obtained from ghg\_inventory\_by\_sector\_all\_00-16.xlsx, available at <https://ww2.arb.ca.gov/ghg-inventory-archive>.

2. 2015 emissions in Tg C yr<sup>-1</sup>, from Vulcan 3.0, Vulcan Project, courtesy, Kevin Gurney, PI.

3. Southern California defined as counties of Los Angeles, Orange, Riverside, San Bernardino, and Ventura.

4. Electricity values from CARB inventory are "in-state" only; no out of state production emissions are included.

5. On-road ratio defined as bio/(fossil+bio), because Vulcan 3.0 includes biofuel (biodiesel and ethanol) in its on-road emission totals.

6. "Transport/Aviation" from the CARB inventory is matched with "Total Airport" in Vulcan.

7. "Transport/Water-borne" from the CARB inventory is being matched with CMV (Commercial Marine Vessel) in Vulcan.

8. Cement (clinker production) is in CARB sector 'Industrial'. Here, we are subtracting it from Industrial and using it in Vulcan category 'Cement'.

The purpose of Table S2 is to detail the values used in arriving at the "total" biofuel:fossil-fuel emission ratio of 0.103 we use for Southern California. The ratio of 0.103 is the quotient 4.718/45.72 and represents the ratio for Southern California, not the state, despite the column heading above 0.103. For each sector, we know the state bio:fossil ratio from the CARB inventory and the Southern California fossil fuel emissions from Vulcan 3.0. By taking the product of the value in "State Bio:Fossil" and "So. Cal. Fossil", we estimate the Southern California biofuel emissions ("So. Cal. Bio."). The fossil fuel and biofuel emissions for Southern California are each totaled to arrive at emissions of 45.72 Tg C yr<sup>-1</sup> and 4.718 Tg C yr<sup>-1</sup>, respectively.

**Table S3. Biogenic:Fossil emission ratios for human respiration and excretion**

<b>County</b>	<b>Population<sup>1</sup></b>	<b>Human<sup>2</sup></b>	<b>Fossil<sup>2,3</sup></b>	<b>Human/Fossil</b>
LA	1.02E+07	1.43	25.77	0.055
Riverside	2.32E+06	0.33	5.68	0.058
San Bernardino	2.12E+06	0.30	3.94	0.076
Ventura	8.53E+05	0.12	8.66	0.014
Orange	3.16E+06	0.44	1.68	0.264
Total	1.86E+07	2.62	45.72	0.057

1. Population data for Jan. 1, 2015 from:

[http://www.dof.ca.gov/Forecasting/Demographics/Estimates/; E-4\\_2019InternetVersion.xls](http://www.dof.ca.gov/Forecasting/Demographics/Estimates/; E-4_2019InternetVersion.xls)

2. Emissions in Tg C yr<sup>-1</sup>.

3. Vulcan 3.0 data courtesy Vulcan Project, Kevin Gurney, PI. Vulcan totals include biogenic CO<sub>2</sub> in on-road transport sector. We have corrected to fossil-only using biogenic:fossil on-road ratios from state of CA inventory.



## References

1. K. R. Verhulst *et al.*, Carbon dioxide and methane measurements from the Los Angeles Megacity Carbon Project – Part 1: calibration, urban enhancements, and uncertainty estimates. *Atmos. Chem. Phys.* **17**, 8313-8341 (2017).
2. C. K. Gately, L. R. Hutyra, Large Uncertainties in Urban-Scale Carbon Emissions. *Journal of Geophysical Research: Atmospheres* **122**, 11,242-211,260 (2017).
3. Y. T. Prairie, C. M. Duarte, Direct and indirect metabolic CO<sub>2</sub> release by humanity. *Biogeosciences* **4**, 215-217 (2007).
4. S. Newman *et al.*, Toward consistency between trends in bottom-up CO<sub>2</sub> emissions and top-down atmospheric measurements in the Los Angeles megacity. *Atmos. Chem. Phys.* **16**, 3843-3863 (2016).
5. E. B. Wetherley, J. P. McFadden, D. A. Roberts, Megacity-scale analysis of urban vegetation temperatures. *Remote Sensing of Environment* **213**, 18-33 (2018).
6. C. Dimiceli *et al.*, MOD44B MODIS/Terra Vegetation Continuous Fields Yearly L3 Global 250m SIN Grid V006 [Data set]. <https://doi.org/10.5067/MODIS/MOD44B.006>.
7. K. W. Thoning, P. P. Tans, W. D. Komhyr, Atmospheric carbon dioxide at Mauna Loa Observatory 2. Analysis of the NOAA GMCC data, 1974-1985. *J. Geophys. Res.* **94**, 8549-8565 (1989).
8. D. York, N. M. Evensen, M. L. Martínez, J. De Basabe Delgado, Unified equations for the slope, intercept, and standard errors of the best straight line. *American Journal of Physics* **72**, 367-375 (2004).
9. R. Wehr, S. R. Saleska, The long-solved problem of the best-fit straight line: application to isotopic mixing lines. *Biogeosciences* **14**, 17-29 (2017).

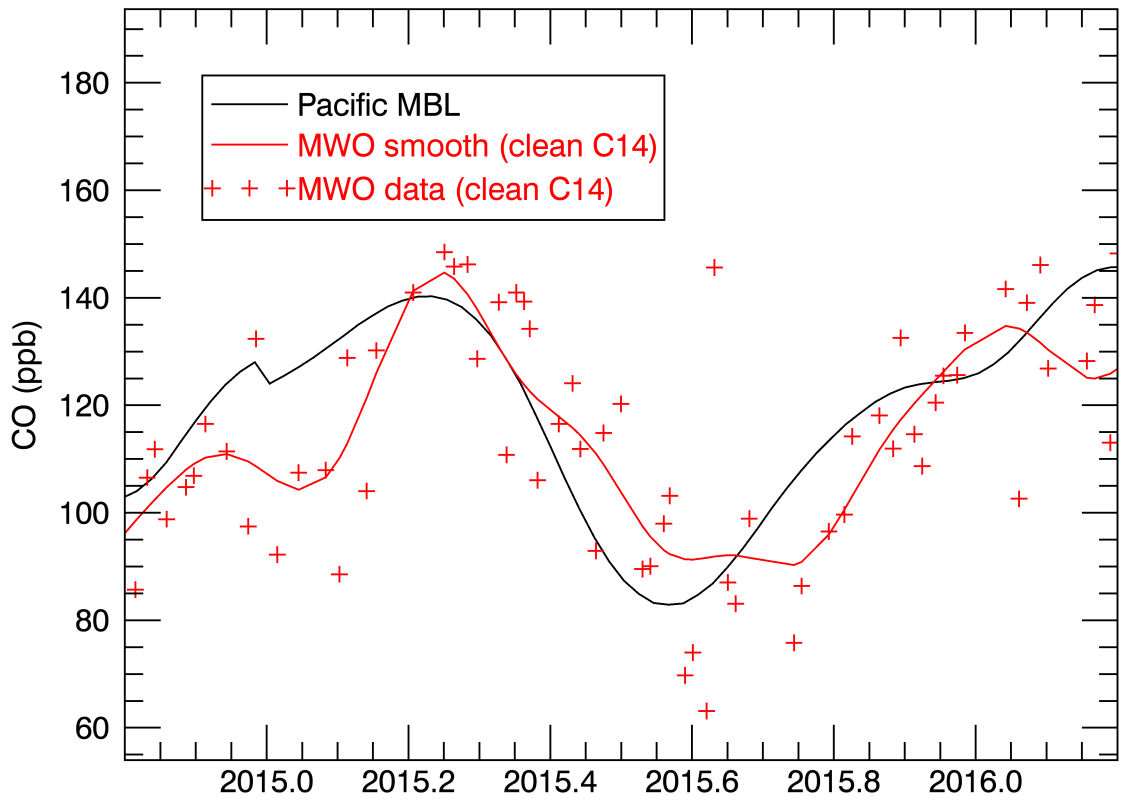


**Figure S1.** Smooth curves for a) 33.4°N in the Pacific Marine Boundary Layer average (black) at nearly the same latitude as MWO (34.2°N) and b) nighttime MWO air samples that were also selected to construct the  $\Delta^{14}\text{C}$  background curve (red). The red crosses represent the MWO data used in the curve fit. The curve fits are calculated using the approach of Thoning et al. (1987) as described in the SI.

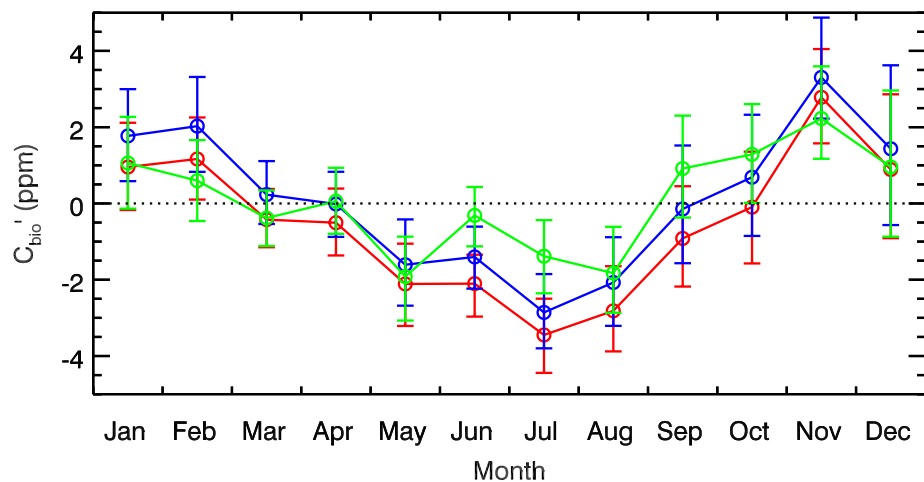


**Figure S2.** The sensitivity of  $C_{\text{bio}}$ ' to various assumptions. The red line represents the baseline monthly  $C_{\text{bio}}$ ' values as in Figure 4; the blue line represents  $C_{\text{bio}}$ ' calculated using the modified bio:fossil emission ratio for fuel sectors of 0.050 (using the ACES inventory); green represents using the site NWR as a background site for  $\text{CO}_2$  and  $\Delta^{14}\text{C}$  instead of MWO. Error bars are 95% confidence intervals, calculated as discussed in the SI text for baseline case.

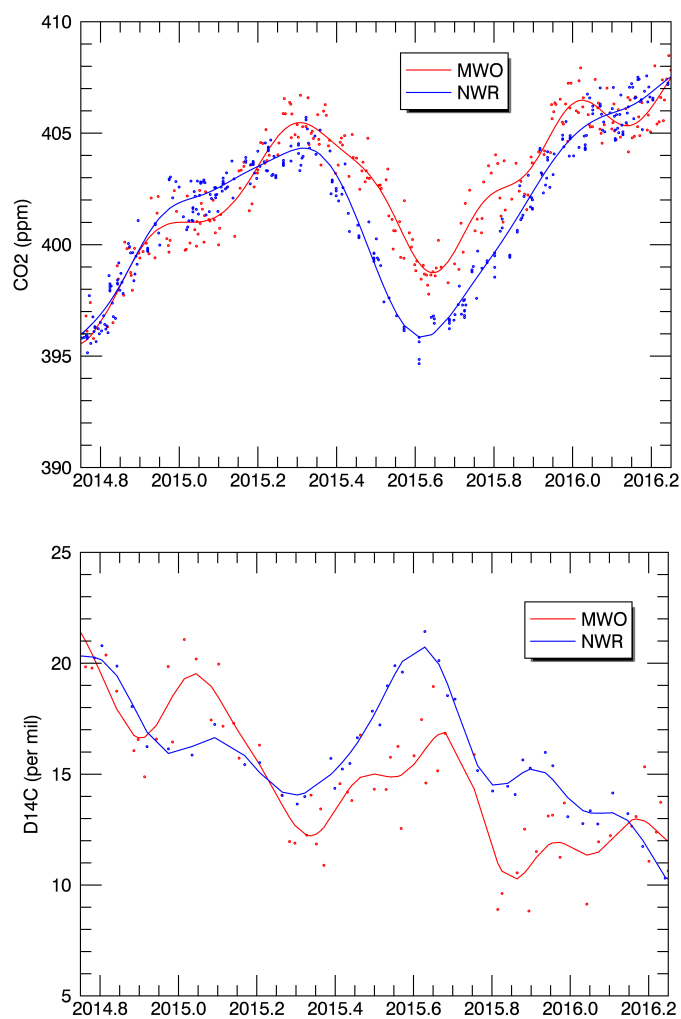


**Figure S3.** Background curve fits (lines) and data used to construct them (small circles) for MWO (red) and NWR (blue) for both CO<sub>2</sub> and  $\Delta^{14}\text{C}$ . Note that MWO symbols and curves are the same as the black crosses and curves shown in Figure 2.

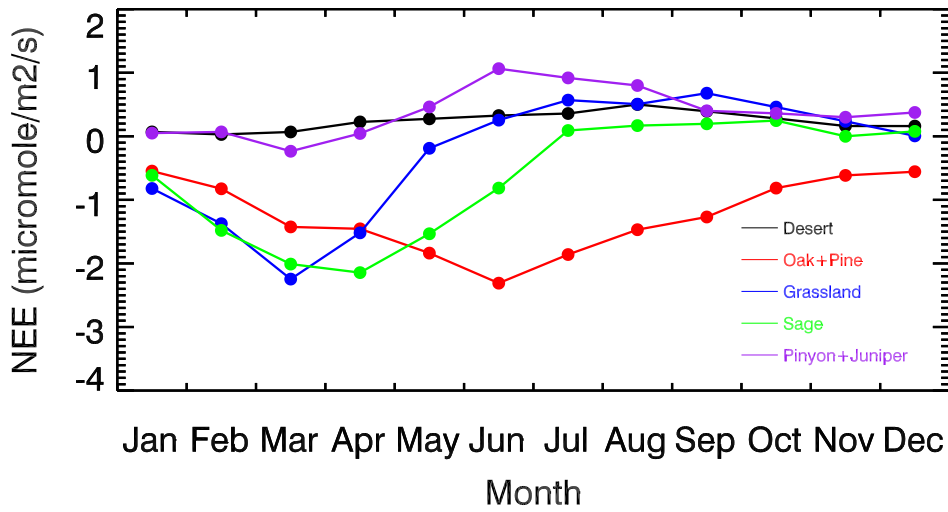


**Figure S4.** Eddy covariance-based Net Ecosystem Exchange (NEE) for five sites in the Southern California Climate Gradient study. Symbols represent monthly averages between 2006 and 2016 for each month, depending on the site. See SI text for details.

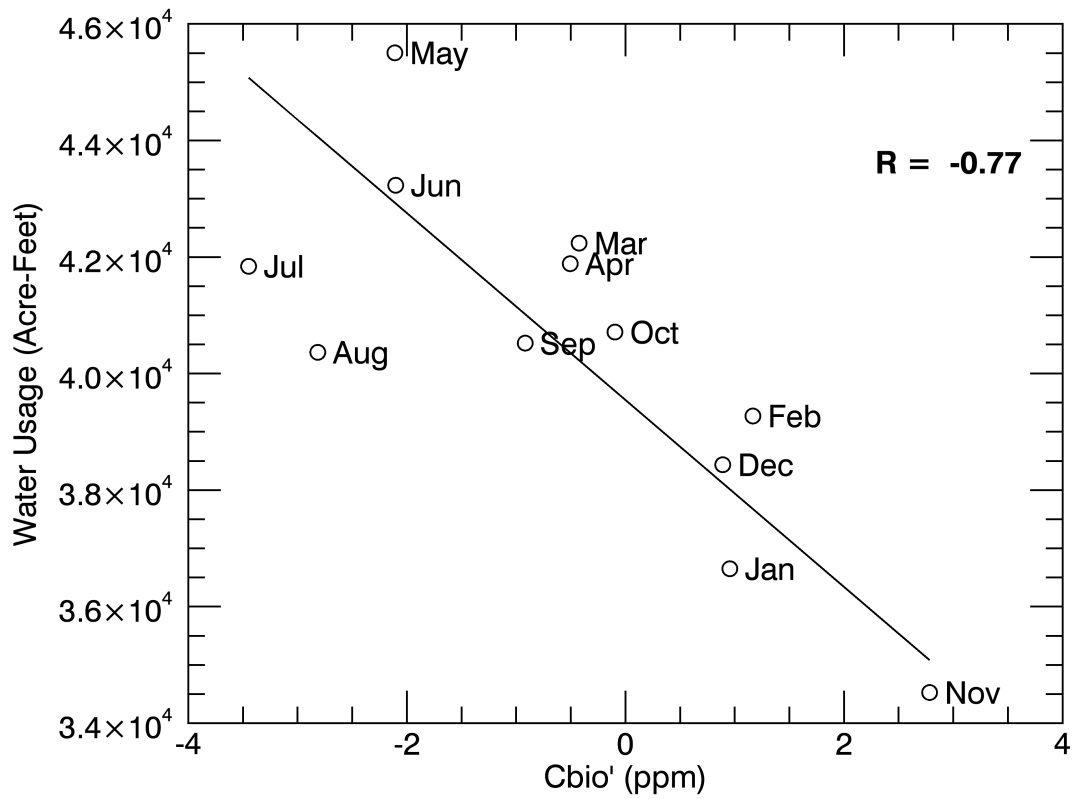


**Figure S5.** Monthly mean  $C_{bio}'$  (from Figure 4) regressed against city of Los Angeles (L.A. Dept. of Water and Power) water usage for 2015. Note that the maximum correlation between the monthly time series occurs at lag = 0. With  $C_{bio}'$  lagging by a month,  $R = -0.33$ ; with  $C_{bio}'$  leading by a month,  $R = -0.65$ .

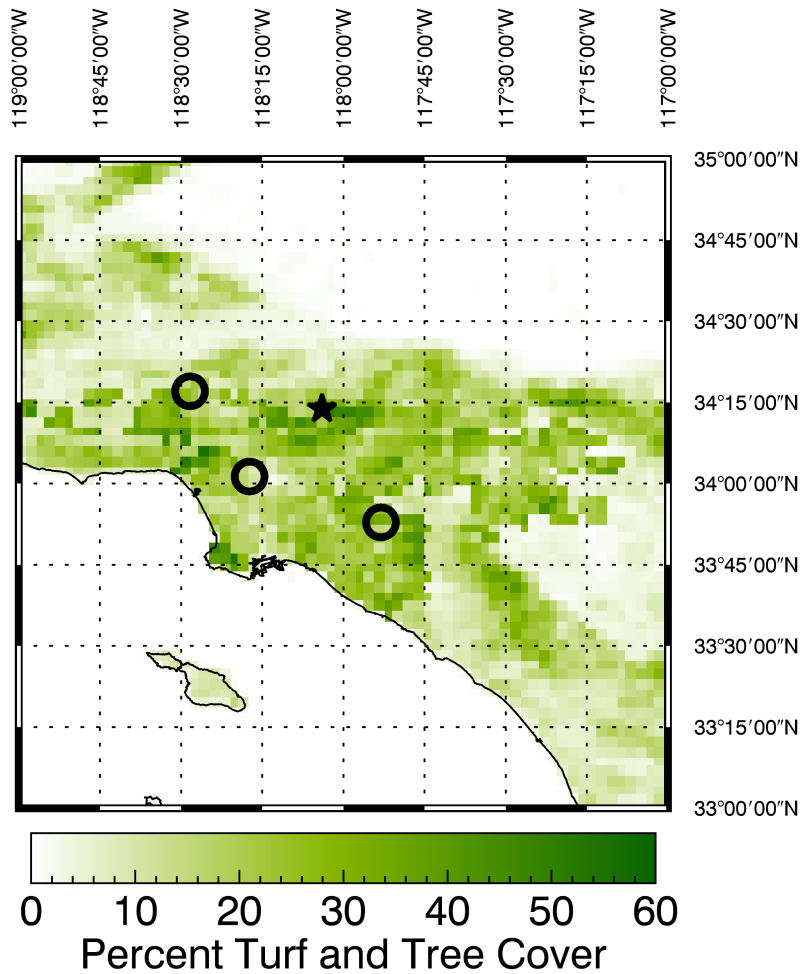


**Figure S6.** Percent tree and turf cover from AVIRIS within the Los Angeles urban area and MODIS Vegetation Continuous Fields (% tree cover and % non-tree vegetation) elsewhere, regridded to the  $0.03^\circ \times 0.03^\circ$  resolution of our footprints. See SI text section “Tree and Turf Cover” for details. The circles and star represent the “signal” and “background” sites used in the study (see Figure 1, main text).

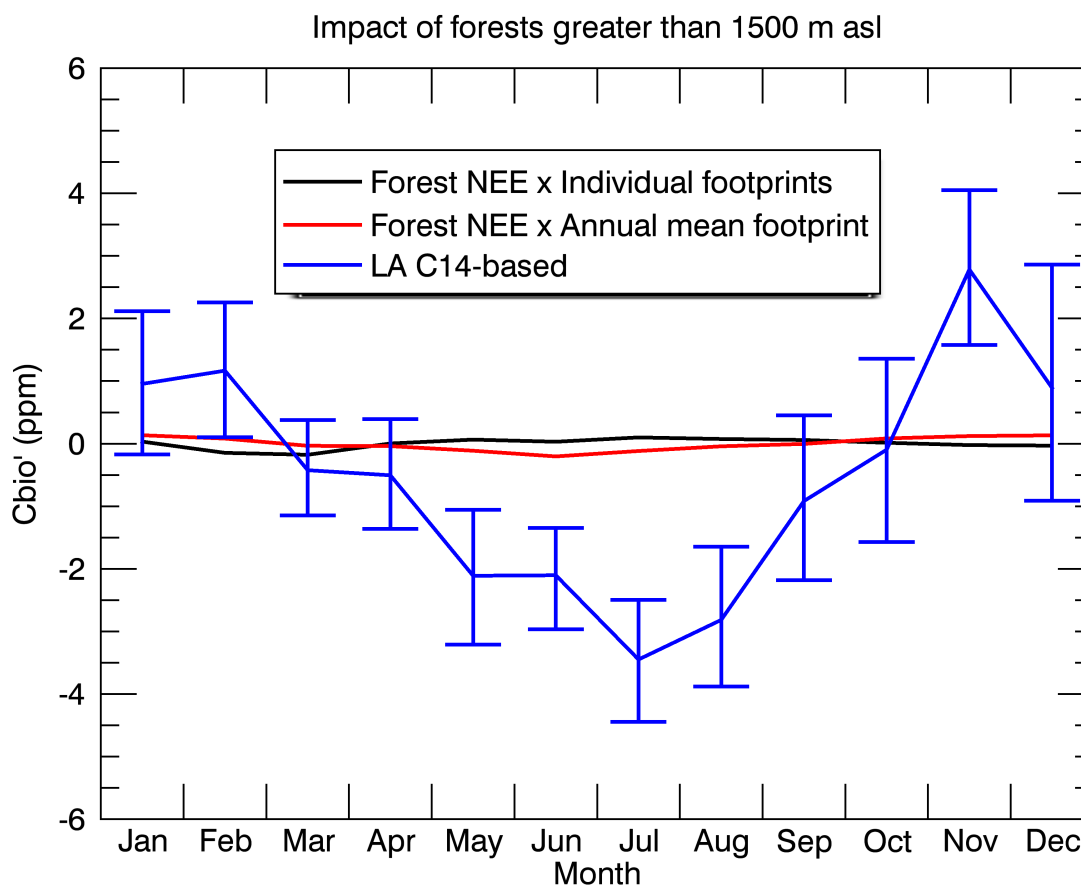


**Figure S7.** Comparison of  $C_{bio}'$  as inferred from Los Angeles  $\Delta^{14}C$  and  $CO_2$  measurements (blue line; identical to that in Figure 4) with locally added biospheric  $CO_2$  from high altitude forest ecosystems within the footprint of GRA, USC and FUL (red and black lines). See SI text for details.



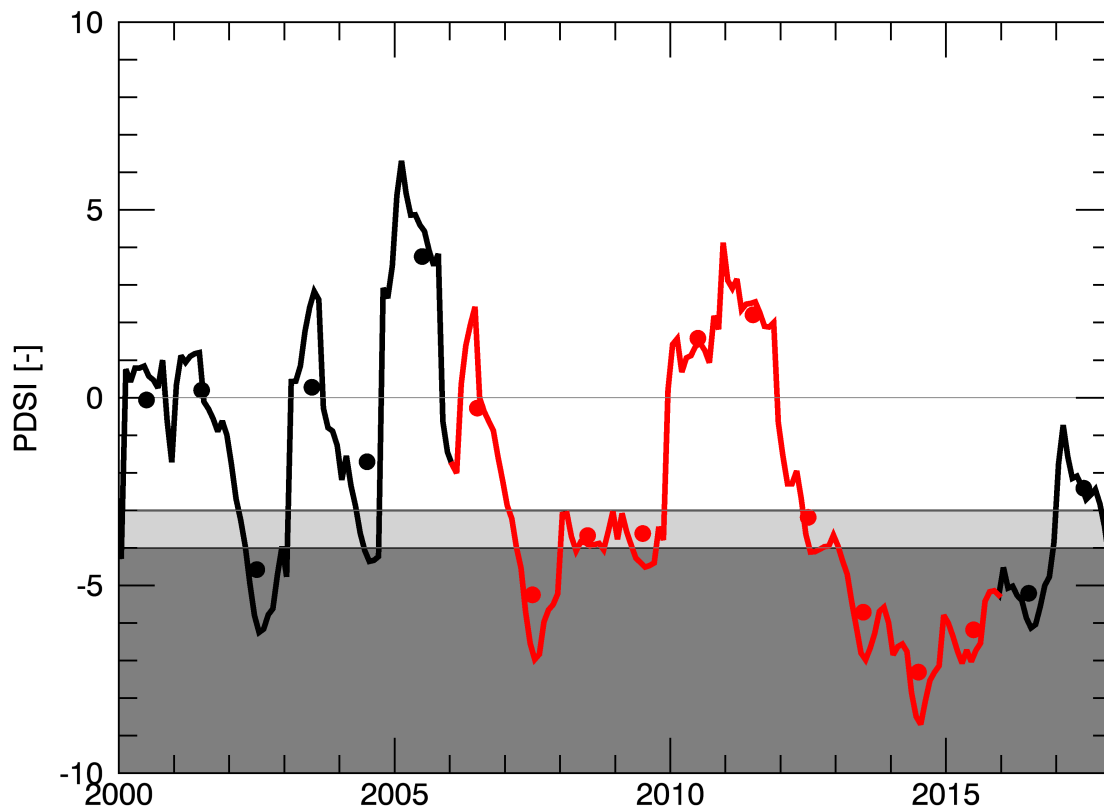


**Figure S8.** Palmer Drought Severity Index (PDSI) for California’s South Coast District between 2000 and 2019 (<https://www1.ncdc.noaa.gov/pub/data/cirs/climdiv/climdiv-pdsidv-v1.0.0-20200604>). The line shows monthly values and the filled circles, annual means. The period 2006-2015 corresponding to the Pasadena (CIT)  $\Delta^{14}\text{C}$  time series is shown in red. Values below -4 are considered “extreme drought” (light grey shading) and values between -3 and -4 are considered “severe drought” (dark grey shading). Between 2000 and 2019, 10 of the 19 years were severe or extreme droughts in the South Coast District.

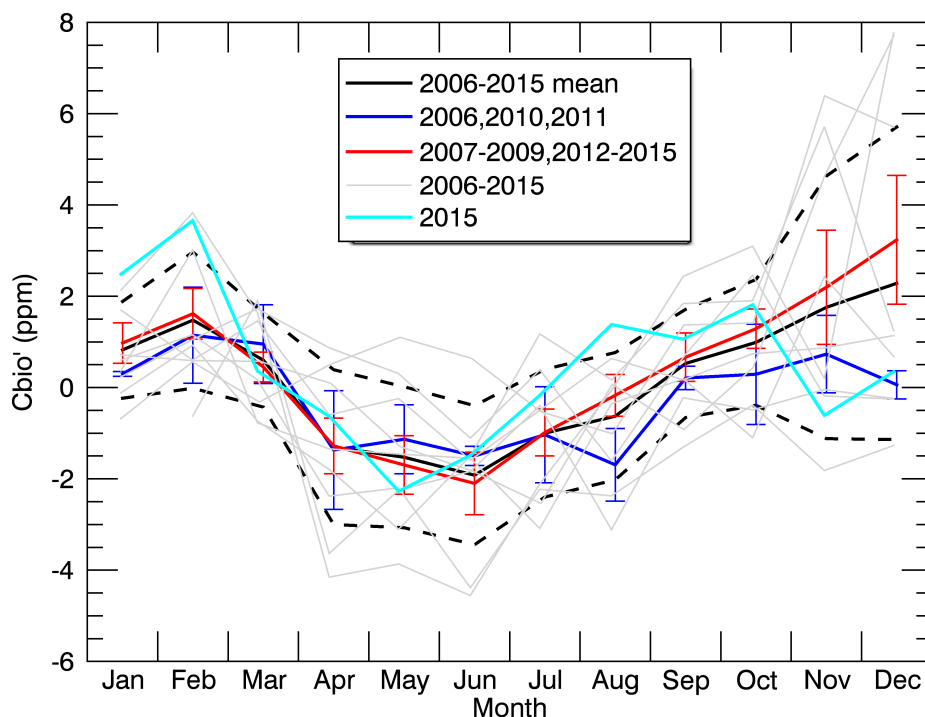


**Figure S9.** Monthly average  $C_{bio}'$  from CIT (California Institute of Technology campus in Pasadena, CA, 10 m agl) between 2006 and 2015. The black solid line represents the 10-year mean, with the black dashed line representing the 1-sigma standard deviation. The grey lines are each year between 2006 and 2015, and the cyan line is 2015, which falls within the one-sigma standard deviation in 9 of 12 months. The blue and red lines represent, respectively, years with PDSI above and below -3 (See Figure S8). The error bars on the red and blue lines represent the standard error of the mean (standard deviation/ $\sqrt{(\text{nyears})}$ , where  $\text{nyears} = 3$  or  $7$ ). Only three of the 12 blue and red error bars do not overlap. Two-tailed student's t-tests performed on the mean amplitude and mean minimum month of the blue and red curves, comparing the very dry and less dry years, show no significant difference even at  $p = 0.10$ .

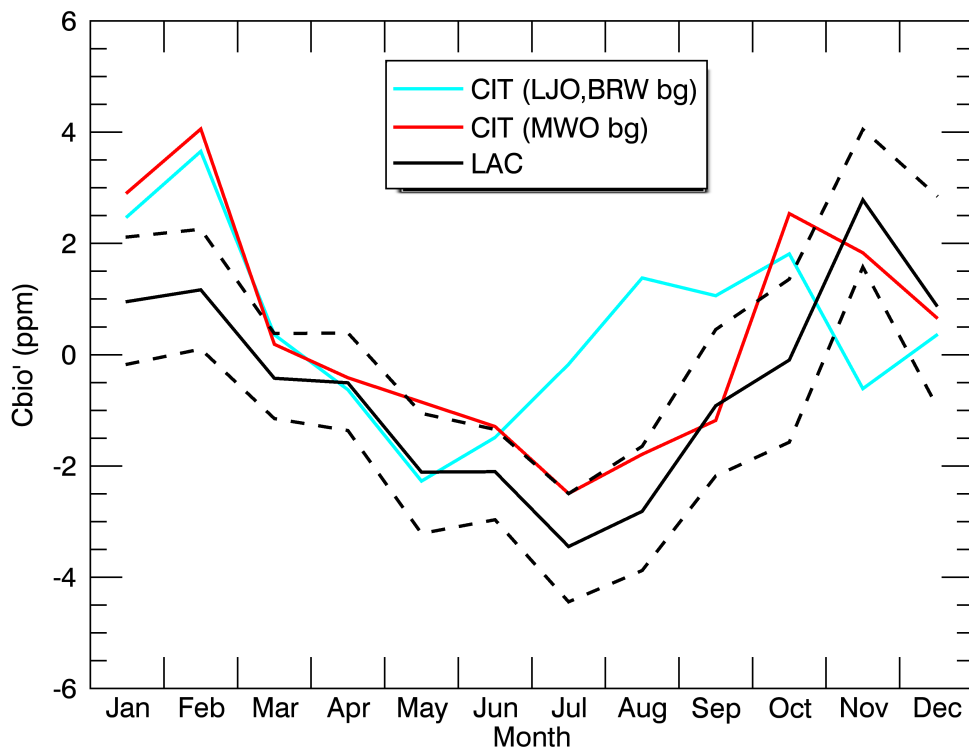


**Figure S10.** Monthly average  $C_{bio}'$  from CIT and L.A. Megacity Project sites (LAC) for 2015. The cyan curve is as in Figure S9, showing the  $C_{bio}'$  calculated using La Jolla, California (LJO) for  $CO_2$  background and Utqiagvik, Alaska (BRW) for  $\Delta^{14}C$  background as for all 10 years shown in Figure S9. The red curve shows  $C_{bio}'$  from CIT recalculated using MWO for both  $CO_2$  and  $\Delta^{14}C$  background, as we do for all L.A. Megacity sites. The black solid line is the  $C_{bio}'$  from the main text with the 95% confidence intervals here portrayed as dashed lines.